Electronic Supplementary Material (ESI) for Green Chemistry.
This journal is © The Royal Society of Chemistry 2022

Electronic Supplementary Information (ESI)

Molecular firefighting biocomposites toward their life-cycle management: fabrication, use and upcycling

Chi Huang[†, §], Ze-Yong Zhao[*, †], Cong Deng[†], Wei Lin[§], Yu-Zhong Wang[*, †]

* Corresponding authors

Ze-Yong Zhao, Tel. & Fax: +86-028-85410755, E-mail: zeyongzhao@scu.edu.cn.

Yu-Zhong Wang, E-mail: yzwang@scu.edu.cn.

† Collaborative Innovation Center for Eco-Friendly and Fire-Safety Polymeric Materials (MoE), State Key Laboratory of Polymer Materials Engineering, National Engineering Laboratory of Eco-Friendly Polymeric Materials (Sichuan), Sichuan University, Chengdu 610064, China

§ College of Biomass Science and Engineering, Key Laboratory of Leather Chemistry and Engineering of Ministry of Education, Sichuan University, Chengdu 610065, China

E-mail: zeyongzhao@scu.edu.cn; yzwang@scu.edu.cn.

ORCID

Ze-Yong Zhao: 0000-0001-8899-9151

Chi Huang: 0000-0003-2966-6255

Figures

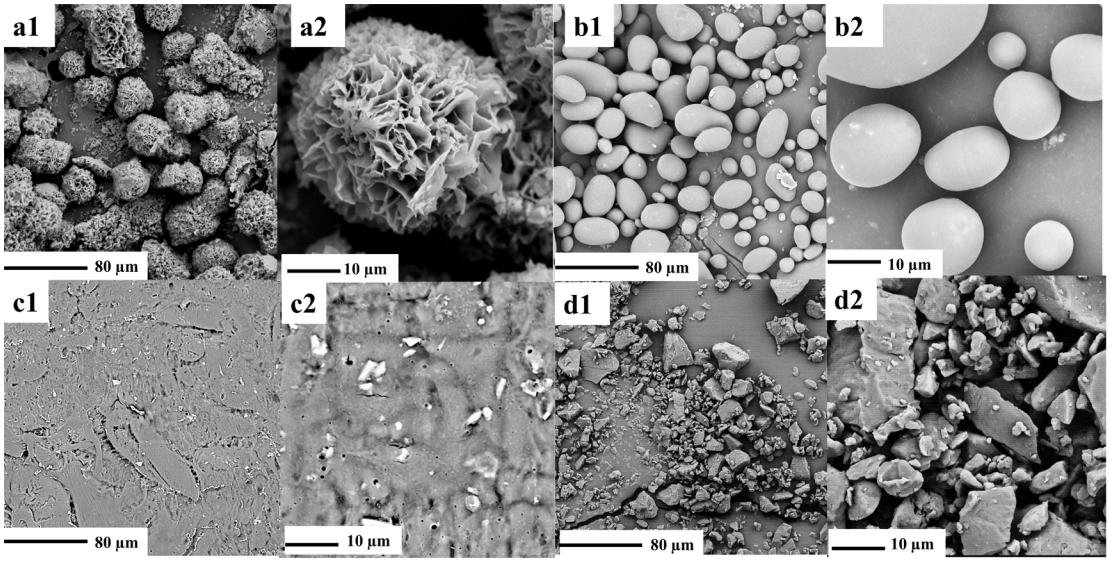

Fig. S1 The SEM images of MPA (a1, a2), PS (b1, b2), PSd (c1, c2) and MPAPS (d1, d2).

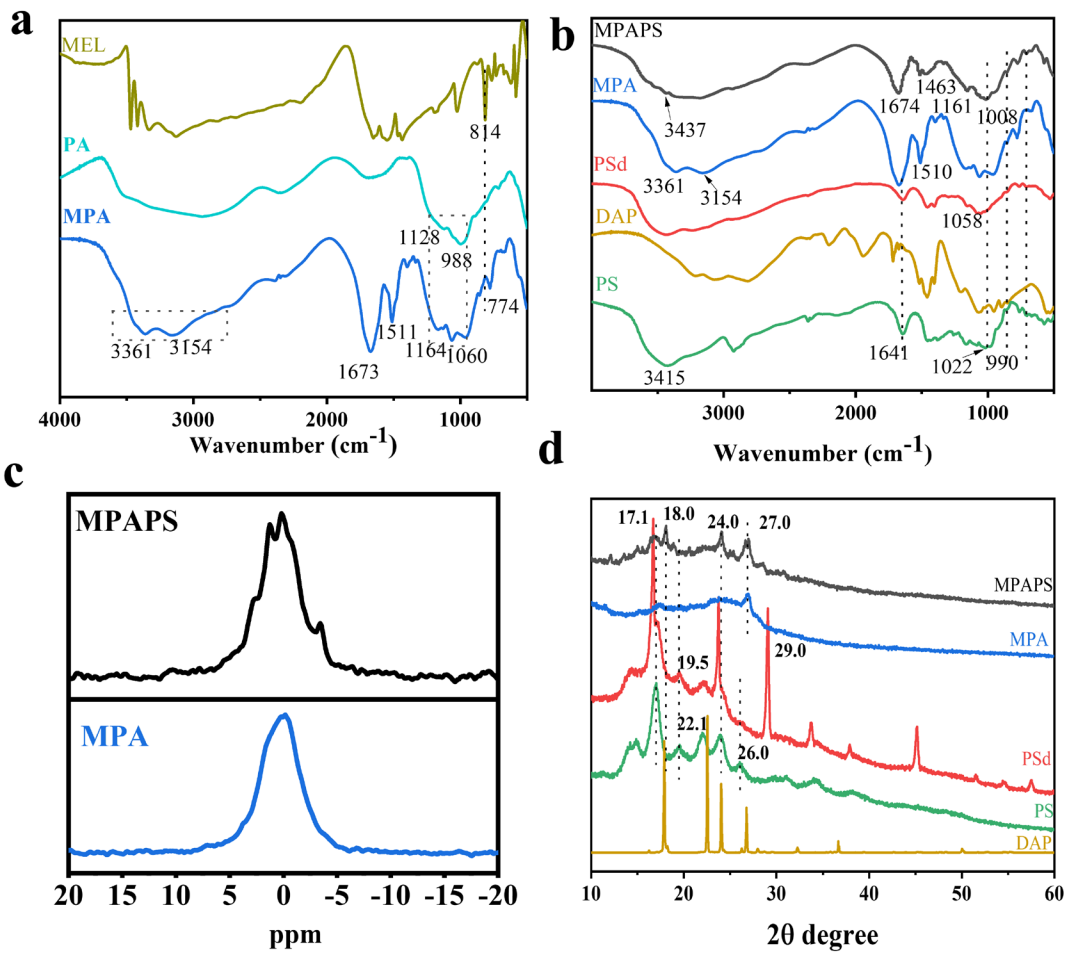

Fig. S2 the FTIR (a, b), solid-state ^{31}P NMR (c) and XRD (d) spectra of raw and synthetic materials.

FTIR The chemical structure of raw and synthetic materials were analyzed by FTIR (Fig. S2a). The peak at 814 cm^{-1} in melamine attributable to the triazine ring vibration shifted to 774 cm^{-1} in MPA, a token of the protonation and deformation of the triazine units [1]. Due to the formation of hydrogen banding, the peaks at 988 and 1128cm^{-1} [1] in PA assigned to phosphoric acid groups shifted to 1060 and 1164 cm^{-1} in MPA [1, 2]. In addition, a new peak emerged at 1511 cm^{-1} was corresponded to the protonated amine [3, 4]; Meanwhile, the new broadband appeared around the regions of 3154-3361 cm^{-1} were assigned to the formation of -NH_3^{+-}O- ionic bonds [5, 6]. Therefore, the MPA was

synthesized via hydrogen bonding and electrostatic interaction.

For PS (Fig. S2b), several characteristic peaks at 3600–3100 cm^{-1} (O–H), 1641 cm^{-1} (intramolecular hydrogen bonding), 1257 cm^{-1} (−O–C(O)– and C–OH), 1167, 1088 and 990 cm^{-1} (C-O-C) [7, 8], 925, 861, 710, 614 and 578 cm^{-1} (pyranose ring) were observed [8]. Compared to the spectrum of PS, the peaks between 990 and 1022 cm^{-1} in PSd spectrum changed due to the rearrangements of the PS after treated with DAP [9]. The peak around 990 cm^{-1} related to the structure crystalline domains of in PS was weakened obviously in PSd, indicating the introduction of DAP could weaken the intramolecular hydrogen bonding of PS [10, 11]. For MPAPS, the characteristic peaks from both PSd and MPA were retained, the broadband appeared between 3400-3100 cm^{-1}, which was attributed to the formation of intermolecular hydrogen bond between PSd and MPA[7 12].The peak at 1674 cm^{-1} was assigned to the P-O from MPA. Notably, a new peak at 1008 cm^{-1} in MPAPS was observed due to the formation of new P-O-C (C_6P–OH) [13, 14], indicating the formation of phosphorylated starch [15].

NMR To further confirm the chemical structure of MPAPS, solid-state ^{31}P NMR was performed (Fig. S2c**)**, the broad resonance signal around 0 ppm of MPA and MPAPS related to phosphate functional groups (PO_4 tetrahedra) [14]. By contrast, the sharp signals appeared in the range from 0 to 5 ppm were ascribed to the presence of the starch phosphates [16, 17].

XRD The XRD analysis were employed to investigate the crystalline structure of raw materials, synthetic materials. In Fig. S2d, the characteristic crystalline peak of starch were found at 17.1, 19.5, 22.1, 24.0 and 26.0°[18]. Compared with the pattern of

PS, the PSd pattern was inclined to be less resolved, and some starch characteristic peaks like 26.0° even disappeared, it was speculated that the intermolecular hydrogen bonds of starch molecules were destroyed partially. For MPA, there was no obvious peaks except for a sharp peak at 27.0°, indicating the MPA in the amorphous phase, the peak at 27° was brought about the π - π stacking formed by the conjugated aromatic system from triazine structure of melamine [19]. On the other hand, MPAPS showed starch characteristic crystallization peak with low resolution at 17.1 and 24.0°, and a π-π stacking peak at 27.0°[19]. It demonstrated that the introduction of MPA further destroys the intermolecular hydrogen bonds in starch, thereby forming more amorphous structures.

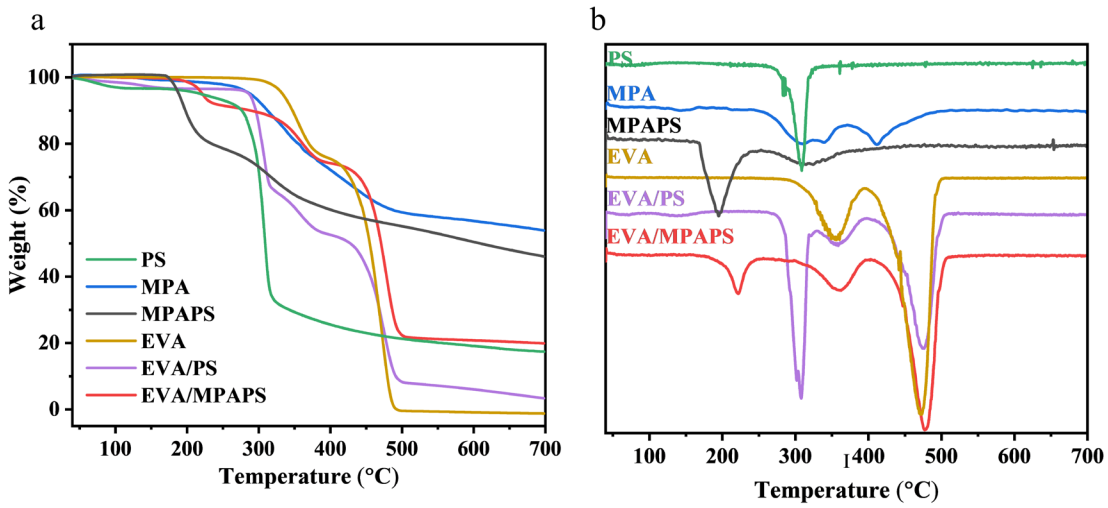

Fig. S3 The TGA (a) and DTG (b) curves of PS, MPA, MPAPS, EVA and its composites (40 wt%) in N_2.

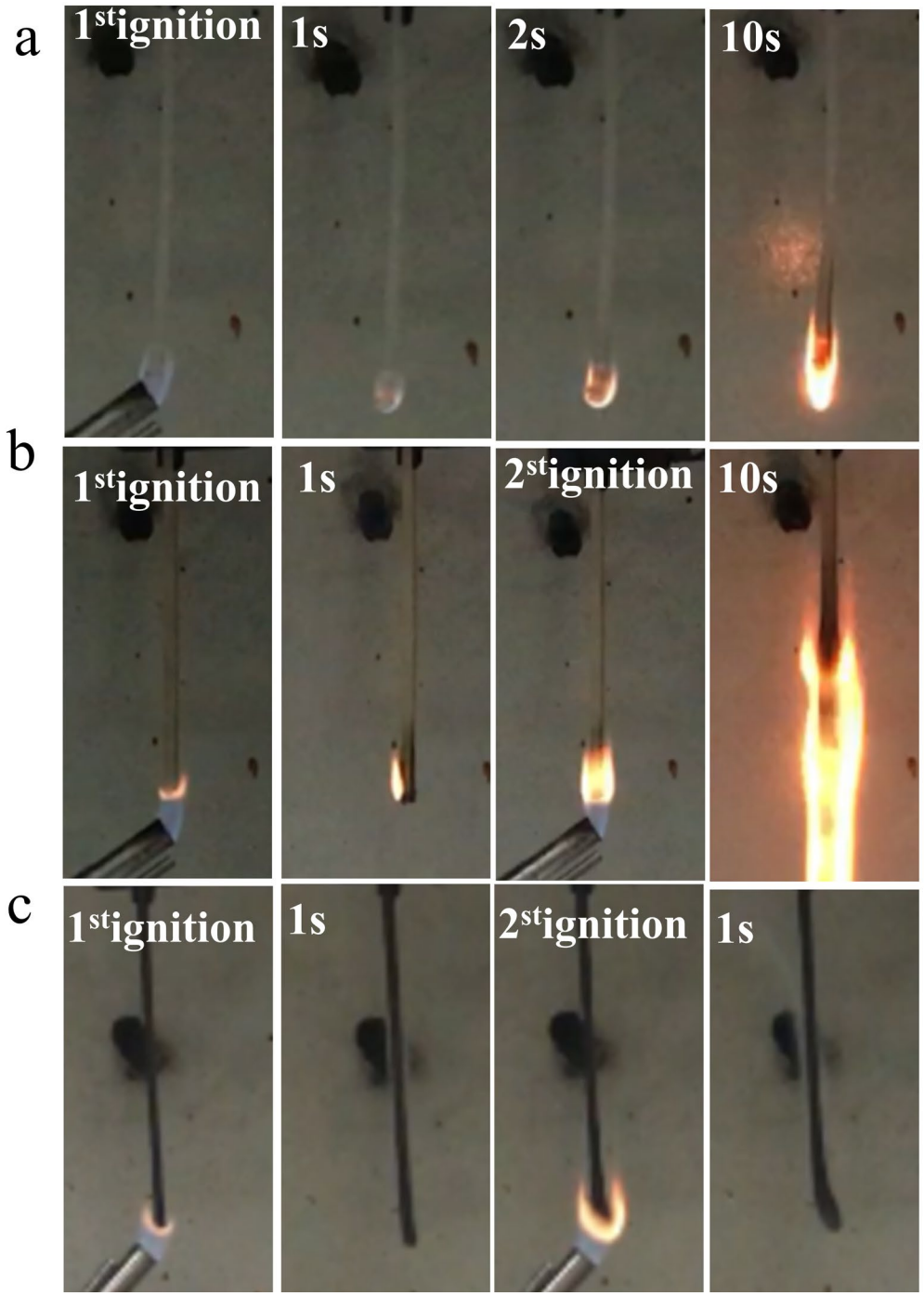

Fig. S4 Video snapshots obtained from vertical burning tests of (a) EVA, (b) EVA/PS (40 wt%) and (c) EVA/MPAPS (40 wt%).

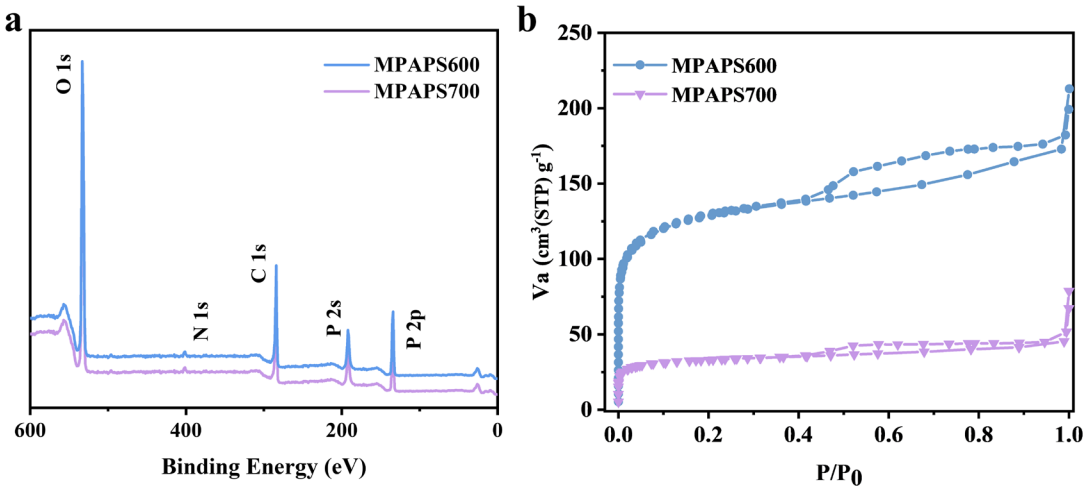

76

77 **Fig. S5** The XPS survey spectra (a) and N_2 adsorption/desorption curves (b) of

78 MPAPS600 and MPAPS700.

79

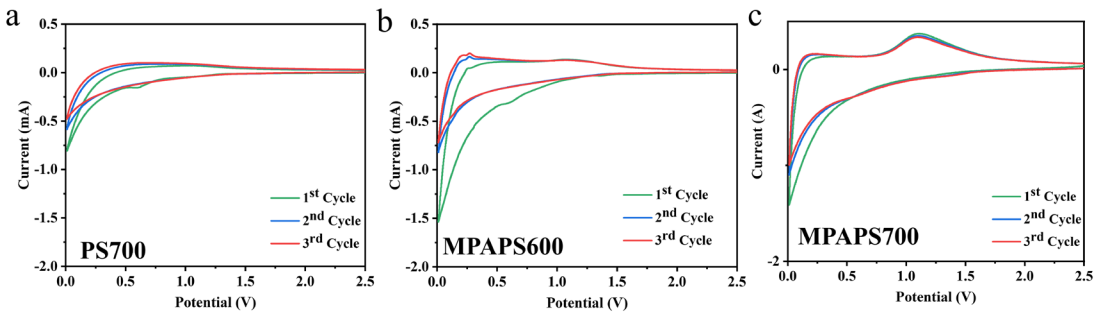

Figure S6 The CV curves of PS700 (a), MPAPS700 (b) and MPAPS600.

Tables

Table S1 The detail data of elongation at break and the tensile strength of EVA and its composites.

Samples	Elongation at Break (%)	Tensile Strength (MPa)
EVA	1251.9±48.9	13.8±0.5
EVA/PS 40 wt%	799.0±18.2	7.3±0.2
EVA/PS 50 wt%	682.6±61.5	4.7±0.3
EVA/MPAPS 40 wt%	844.2±38.3	9.3±0.5
EVA/MPAPS 50 wt%	762.9±99.7	4.8±0.3

Table S2 The TGA and DTG data of PS, MPA, MPAPS, EVA and its composites (40 wt%) in N_2.

Samples	$T_{5\%}$(°C)	T_{max1}(°C)	T_{max2}(°C)	T_{max3}(°C)	Residue at 700°C (%)
PS	219.4	308.3			17.4
MPA	290.2	309.6	409.8		52.9
MPAPS	188.5	194.7	315.0		46.1
EVA	333.3	356.3	473.1		0.0
EVA/PS	292.3	308.3	360.7	479.4	6.7
EVA/MPAPS	221.3	222.2	358.6	477.2	19.9

Table S3 The results of EVA and its composites from LOI and UL-94 test.

Samples	UL-94	Dripping	LOI (%)
EVA	NR	YES	19.0±0.5
EVA/PS (40 wt %)	NR	YES	20.5±0.6
EVA/PS (50 wt %)	NR	NO	21.0±0.5
EVA/MPAPS (40 wt %)	V0	NO	26.6±0.4
EVA/MPAPS (50 wt %)	V0	NO	27.8±0.5

Table S4 The results of EVA and its composites from CCT test.

Samples	TTi (s)	PHRR (kW/m^2)	THR (MJ/m^2)	Peak SPR (m^2/s)	Mean EHC (MJ/kg)
EVA	30	1234.6	107.2	0.12	35.8
EVA/PS (40 wt %)	13	979.2	105.5	0.13	29.5
EVA/MPAPS (40 wt %)	12	250.5	77.7	0.05	26.1

Table S5 Textural parameters of MAPAPS600 and MPAPS700 obtained from N_2 adsorption/desorption measurement.

Samples	S_{BET} ($m^2\ g^{-1}$)	V_m (cm^3 (STP) g^{-1})	Total Pore volume ($cm^3\ g^{-1}$)	Average pore diameter (nm)
MPAPS600	407.6	93.7	0.29	2.0
MPAPS700	104.0	23.9	0.07	2.5

References

1 J. Bai, B. Xi, H. Mao, Y. Lin, X. Ma, J. Feng and S. Xiong, *Advanced Materials*, 2018, **30**, 1802310.

2 H. Peng, D. Wang, M. Li, L. Zhang, M. Liu and S. Fu, *Chem. Eng. J. (Amsterdam, Neth.)*, 2019, **372**, 873-885.

3 Y.-Y. Gao, C. Deng, Y.-Y. Du, S.-C. Huang and Y.-Z. Wang, *Polym. Degrad. Stab.*, 2019, **161**, 298-308.

4 P.-J. Wang, D.-J. Liao, X.-P. Hu, N. Pan, W.-X. Li, D.-Y. Wang and Y. Yao, *Polymer Degradation and Stability*, 2019, **159**, 153-162.

5 H. Nabipour, X. Wang, M. Z. Rahman, L. Song and Y. Hu, *Journal of Cleaner Production*, 2020, **273**, 122832.

6 X. Jin, J. Sun, J. S. Zhang, X. Gu, S. Bourbigot, H. Li, W. Tang and S. Zhang, *ACS Applied Materials & Interfaces*, 2017, **9**, 24964-24975.

7 L. Liu, Y. Yu and P. a. Song, *Industrial & Engineering Chemistry Research*, 2013, **52**, 16232-16238.

8 M. E. Villanueva, A. M. d. R. Diez, J. A. González, C. J. Pérez, M. Orrego, L. Piehl, S. Teves and G. J. Copello, *ACS Applied Materials & Interfaces*, 2016, **8**, 16280-16288.

9 D. Domene-López, J. J. Delgado-Marín, I. Martin-Gullon, J. C. García-Quesada and M. G. Montalbán, *International Journal of Biological Macromolecules*, 2019, **135**, 845-854.

10 V. P. Silva Nykänen, O. Härkönen, A. Nykänen, P. Hiekkataipale, J. Ruokolainen

and O. Ikkala, *Green Chemistry*, 2014, **16**, 4339-4350.

11 M. R. Area, B. Montero, M. Rico, L. Barral, R. Bouza and J. López, *International Journal of Biological Macromolecules*, 2020, **164**, 2028-2037.

12 M. N. Prabhakar, A. u. Rehman Shah and J.-I. Song, *Carbohydrate Polymers*, 2017, **168**, 201-211.

13 J. Zhang and Z.-W. Wang, *Industrial Crops and Products*, 2009, **30**, 105-113.

14 Y. Shi, D. Belosinschi, F. Brouillette, A. Belfkira and B. Chabot, *Carbohydrate Polymers*, 2014, **106**, 121-127.

15 W. Ji, D. Wang, J. Guo, B. Fei, X. Gu, H. Li, J. Sun and S. Zhang, *Carbohydrate Polymers*, 2020, **233**, 115841.

16 L. Passauer, H. Bender and S. Fischer, *Carbohydrate Polymers*, 2010, **82**, 809-814.

17 L. Passauer and H. Bender, *Carbohydrate Polymers*, 2017, **168**, 356-364.

18 M. Zdanowicz, *International Journal of Biological Macromolecules*, 2021, **176**, 387-393.

19 X. Wang, K. Maeda, A. Thomas, K. Takanabe, G. Xin, J. M. Carlsson, K. Domen and M. Antonietti, *Nature Materials*, 2009, **8**, 76-80.